

Recent Developments of the Containment Code ICECO

C.Y. Wang

*Reactor Analysis and Safety Division, Argonne National Laboratory,
9700 South Cass Avenue, Argonne, Illinois 60439, U.S.A.*

Summary

The containment code ICECO developed at the Argonne National Laboratory has been used for the study of containment integrity under HCDA conditions and for the evaluation and interpretation of test results of small scaled experiments. To meet the needs of these objectives, a number of improvements and extensions of the code were made recently. This paper describes these improvements, concerning more specifically, the treatments of multi-materials, complex internal structures adjacent to the core, and the spillage of coolant through the openings of the reactor cover and cover-vessel junction.

A multi-material model is developed to improve the treatment of the inertia of the reactor core as well as the dynamics of high density materials. This model is also applicable to 2-D compressible flows of immiscible fluids, allowing for large distortions at the material interface. The analysis utilizes a control volume technique to solve the conservation equations of mass, momentum, and energy. A modified Poisson equation is derived, which considers volume fractions and surface permeabilities of different materials.

Structural components in LMFBRs usually have small coolant passageways. For example, the core-support diagrid and upper internal structure (UIS) have perforated holes to allow coolant circulation. A technique has been developed in ICECO for analyzing flow through small openings and flow blockage near the perforated structure. This technique has been improved to account for losses due to friction and flow-area change to reduce the conservatism of the previous analysis based on inviscid boundary conditions. This scheme can also be used to calculate the coolant spillage through the penetrations on the reactor cover, if these penetrations are assumed to open under the slug impact force. Thus, the code can adequately calculate coolant-spillage histories and provide information for further calculations of pressure and thermal loading on secondary containment generated from sodium-spray fires.

The structural capability of ICECO is also improved considerably. A 2-D quadrilateral elastic-plastic element has been developed to model solid continuum inside the primary containment. The original formulation of this element were based on the finite-difference method. To facilitate the numerical calculations and the coupling with shell elements, the equations of motion of this element are written in the finite-element format by means of intermediate nodal forces.

Sample problems are used to illustrate these improvements made in the ICECO code, including a comparison of calculational results with SRI complex vessel experiment SM-2.

1. Introduction

The containment code, ICECO, developed at the Argonne National Laboratory has been used for (1) the study of containment integrity under HCDA conditions, (2) the evaluation and interpretation of test results of small scale experiments, and (3) the project supports in the area related to LMFBR safety. The latest development of the ICECO code has been described in Refs. [1-3]. The salient features of the code were the implicit calculation of compressible flows, the generalized treatment of the highly contorted fluid boundaries, the computation of the containment response, as well as the analysis of above-core hydrodynamics and sodium spillages. Development of this code has continued not only in expanding its calculational capabilities, but also in improving its program logic as observed from various comparisons between analytical predictions and experimental data.

Recently, several improvements have been made to the ICECO code in order to refine the analysis of the fluid-structure transient occurring in a typical LMFBR geometry. These improvements include treatments of multi-material flow, the elastic-plastic solid continuum, as well as the flow through porous solid and perforated structures. Furthermore, the hydrodynamic model of perforated structures has been generalized in such a way that coolant spillage through penetrations on the reactor cover can also be calculated. Since the hydrodynamic formulation is done in the Eulerian-coordinate system, the resulting version of the ICECO code would be applicable to problems involving large material distortion, flow around corners and irregularities, and multi-dimensional sliding.

In this paper the finite difference equations and numerical method are described. Sample problems illustrating these analytical developments are given.

2. Multi-Material Interaction

Previous ICECO analyses of the primary-containment response to an HCDA generally considered the reactor core as a gas bubble exerting a uniform pressure at the coolant-bubble interface. The bubble inertia was neglected, and the fluid motion inside the core was not taken into consideration in the numerical analysis. If a reactor core consisting of a material of very small density comparable to that of the coolant, the neglect of core inertia is a good assumption. However, if the reactor core consists of a sodium-gas mixture or other materials with density comparable to the coolant density, ignoring the core inertia and the fluid motion may have undesirable effects on the numerical solution. Moreover, in the vicinity of the core region, the effect of the high-density materials, such as the radial and axial reflectors, on the coolant motion should also be taken into account.

To treat the bubble inertia and multifluid flow, a multi-fluid interaction model was developed. The model is designed to study two-dimensional compressible flows of immiscible fluids, allowing for large-amplitude distortions of the interface. However, interpenetration between materials is not permitted. The mass, momentum, and state equations describing the flow of a heterogeneous, compressible, and viscous fluid are identical to the one-material counterparts, except that the multi-material momentum equation contains a more complicated viscous-diffusion term. These complications are necessary to account for the spatial variation in the coefficients of viscosities due to the presence of different fluids. If viscosity coefficients λ and μ are constant throughout, the momentum equation reduces to the corresponding equation used in the ICE technique [4].

The approach to obtain the difference equation is similar to the ICE technique. Since the fluid motion could change abruptly due to the density discontinuity, a donor-cell dif-

ference scheme has been used. Also, a new flagging scheme is developed to distinguish the cell containing different fluids. Thus, if a mixing cell contains different materials, the values of ρ , λ , and μ must be determined for the cellwise calculations. To account for these physical properties accurately, we use a volume-weighting scheme so that, in the mixing cell,

$$\sum_1^m \alpha_m = 1, \quad \rho = \sum_1^m \alpha_m \rho_m, \quad \lambda = \sum_1^m \alpha_m \lambda_m, \quad \text{and} \quad \mu = \sum_1^m \alpha_m \mu_m, \quad (1)$$

where $\alpha_m = v_m/v_C$ is the material volume fraction, defined as the ratio of the volume occupied by the material m and the volume of that Eulerian cell. The volume v_m is computed according to the position of the boundary curve associated with material m (see Fig. 1), using a scheme developed to compute the intersected volume between two quadrilaterals for rezoning the Lagrangian grids [5].

Through elimination of the advanced-time densities in the mass equation by using the equation of state and the momentum equations, a modified Poisson equation is obtained which has the form

$$p_{i,j}^{n+1} \left[\sum_1^m \left(\frac{\alpha_m}{c_m} \right)_{i,j} + 2\theta\phi\delta t^2 \left(\frac{1}{\delta r^2} + \frac{1}{\delta z^2} \right) \right] = H_{i,j}^n + \theta\phi\delta t^2 \left[\frac{r_{i-(1/2)} p_{i-1,j}^{n+1} + r_{i+(1/2)} p_{i+1,j}^{n+1} + p_{i,j-1}^{n+1} + p_{i,j+1}^{n+1}}{r_i \delta r^2} + \frac{p_{i,j-1}^{n+1} + p_{i,j+1}^{n+1}}{\delta z^2} \right], \quad (2)$$

in which $H_{i,j}^n$ is the source term computed from the previous cycle values of pressures, densities, velocities, and viscous coefficients.

3. Flow Near Perforated Structures

Structural components in LMFBRs usually have small coolant passageways, such as the core-support diagrid, the upper internal structure (UIS), and the reactor cover with penetrations that could become opening under the slug impact force. As a first step toward the full representation of flow through perforated structure a mathematical model was developed and reported in Ref. [2]. In that model the effect of viscosity on the fluid motion is accounted for only in the coolant passageways, but not in the region near the perforated structure. Neglecting the viscous forces in the model can cause faster movement of the coolant near the perforated solids and the reactor cover. As a result, the slug impact loading and the subsequent quantity of sodium ejected are slight overestimated.

To improve the mathematical model, we have incorporated the viscous-stress tensor into the momentum equations. In the analysis the basic equations are derived using the control volume technique. The underlying idea is to account for the actual fluid volume and the available flow areas of the perforated structure in the formulation [6,7]. For instance, at the exit of a perforated structure the radial momentum equation can be derived using control volume ABCDEF shown in Fig. 2 and has the form

$$\frac{(\rho u)_{i+1/2,j}^{n+1} + (\rho u)_{i+1/2,j}^n}{\delta t} = \frac{1}{\delta r} (\bar{p}_{i,j} - \bar{p}_{i+1,j}) + R_{i+1/2,j} \quad , \quad (3)$$

where

$$R_{i+1/2,j} = R_C + \frac{1}{\delta r} (q_{i,j} - q_{i+1,j}) + g_r \rho_{i+1/2,j} + \frac{\mu}{\delta z} \left[\frac{u_{i+1/2,j+1} - u_{i+1/2,j}}{\delta z} - \frac{v_{i+1,j+1/2} - v_{i,j+1/2}}{\delta r} - \frac{u_{i+1/2,j} - u_{i+1/2,j-1}}{\delta z} + \frac{\phi_{i+1} \tilde{v}_{i+1,j-1/2} - \phi_i \tilde{v}_{i,j-1/2}}{\delta r} \right] ,$$

is the source term; R_C is the term due to fluid convection [2] that includes effect of flow-area change; q is the viscous pressure; ϕ is the perforation ratio; \tilde{v} is the velocity in the coolant passageway; \bar{p} is the advanced-time pressure; μ is the viscous coefficient.

As can be seen from eq. (3) that the losses due to viscous dissipation can simply be included in the source term of the momentum equation. Thus, the inclusion of effects due to viscosity, and flow-area change appears to be a simple modification of the source-term calculation.

4. Elasto-Plastic Solids

The finite element approach is used in the analysis of response of solid media inside the primary containment. A quadrilateral element is developed to model the elastic-plastic solids, such as the radial shield and lead. Both geometric and material nonlinearities are considered in the calculation. The equation of motion are integrated explicitly and has the form [8]

$$M \ddot{\underline{u}} = \underline{F}^{ext} - \underline{F}^{int} \quad , \quad (4)$$

where M is the mass matrix; \underline{u} the displacement; \underline{F}^{ext} the discretized external forces; and \underline{F}^{int} the discretized internal forces.

The external forces are the pressure forces transmitted from the fluids. These forces are supplied by the fluid-dynamic calculation. The internal forces can be computed from the finite-difference representations using four quadrilaterals shown in Fig. 3, similar to the method of Wilkins [9]. To facilitate the treatment of the boundary conditions and the arbitrary combination of the solid and thin shell elements the equation of motion are written through the use of the intermediate nodes forces of each element. Thus, for a typical element shown in Fig. 4, the internal nodal forces in the r and z directions at node 1 are:

$$(F_1)_r^{int} = 1/2 [\sigma_{rr} (z_2 - z_4) - \sigma_{rz} (r_2 - r_4)] \bar{r} - X \quad ,$$

and (5)

$$(F_1)_z^{int} = - 1/2 [\sigma_{zz} (r_2 - r_4) - \sigma_{rz} (z_2 - z_4)] \bar{r} - Y \quad ,$$

where

$$\bar{r} = \frac{M}{\rho^n A^n} , \quad \phi = 1/4 \sum_{i=1}^4 (A^n \rho^n)_i ,$$

$$X = 1/4 (\sigma_{rr} - \sigma_{\theta\theta}) \frac{\phi}{\rho} , \quad \text{and} \quad Y = 1/4 \sigma_{rz} \frac{\phi}{\rho} .$$

In eq. (5) subscripts r and z denote the internal nodal forces in the radial and axial directions, respectively; M_1 is the mass associated with node 1; ρ is the density; A is the area; σ_{rr} , σ_{zz} , and $\sigma_{\theta\theta}$ are the total stress components in the radial, axial, and circumferential directions, respectively; σ_{rz} is the shearing stress.

Note that the internal nodal forces at nodes 2, 3, and 4 can be obtained in a similar manner. The internal forces at each nodal point is the summation of all the internal forces contributed by its surrounding elements.

5. Results

Because of space limitation only two problems illustrating the application of the development in the multi-material interaction and the elastic-plastic solid are given. Other samples concerning flow through perforated structure and sodium spillage will be presented in the conference.

The first one deals with fluid transient involving two-material interaction. Figure 5 shows a simplified reactor configuration used in this study. The reactor core is considered as a gas bubble with an initial core pressure of 31 MPa. The heavy material surrounding the core and the coolant are represented by two types of marker particles, i.e., diamond and dot, respectively. All the external boundaries are assumed to be rigid and free slip. The core barrel is modeled by four rigid obstacles. To visualize the motion of the material interface, the interfacial particles are connected by straight lines, which move across the fixed Eulerian grids during the motion.

Figure 6 gives the reactor configurations at three different times. These configurations show how the gas bubble expands and how the free surface moves during the excursion. They also show the relative movement between the two fluids. These two fluids undergo large motion, especially in the vicinity of the core barrel. Note that there is no interpenetration between the fluids, since a smooth interface is always maintained throughout the excursion. Figure 5 also revealed that the upper portion of the reactor core is highly distorted following the propagation of the pressure wave generated by the slug impact.

The second problem deals with comparison of ICECO prediction with SRI complex vessel experiment SM-2. The experimental apparatus used in SM-2 is shown in Fig. 7. The cylindrical vessel was made from Ni-200 to simulate the stress-strain relationships of the Type 304 stainless steel at the reactor operating temperature. The core barrel consists of 0.254-cm-thick aluminum cylinder and segmented steel rings, which was simulated as the elastic-plastic material in the ICECO calculation. Other information concerning the experimental instrumentation is given in Ref. [10].

Figures 8 and 9 give comparisons of pressure histories at gauge P5 and the strain histories at gauge SG2, respectively. The agreement between the analytical results and the ex-

perimental measurement is very good. Figure 10 compares the calculated vessel deformation with the posttest measurement. The agreement is exceptionally good, particularly at the lower vessel. The good comparison thus validate the fluid-structure interaction treatment for problem involves complex internals.

6. Conclusions

This paper has described some recent developments made in the ICECO code which greatly enhanced the code calculational capability. A multi-material interaction model is applicable to problems involving large material distortion, multi-dimensional sliding interface, as well as flow around corner and other irregularities. Inclusion of viscous dissipation terms in the momentum equations adjacent to the porous solids and perforated structures is of significance for analyzing the above-core hydrodynamics as well as the sodium-spillage phenomena. The addition of the elastic-plastic solids element is particularly useful in modeling complex internals that usually present in typical reactor containments.

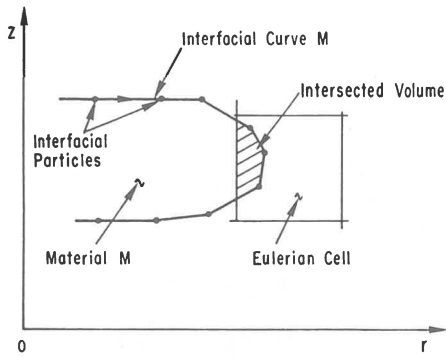
As illustrated in the example problem, the ICECO code predictions have been compared with the experimental results. Good agreement indicates that the ICECO code is an essential tool for analyzing containment response during an hypothetical core disruptive accident.

Acknowledgments

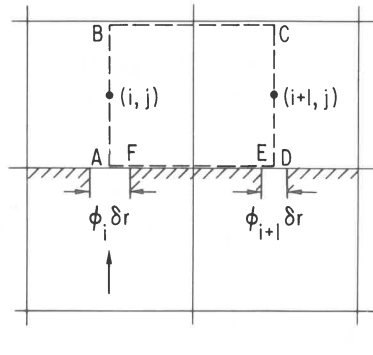
The author would like to thank D. Basinger and W. R. Zeuch for providing programming assistance and test calculation, respectively. This work was performed in the Engineering Mechanics Program of the Reactor Analysis and Safety Division at Argonne National Laboratory under the auspices of the U.S. Department of Energy.

References

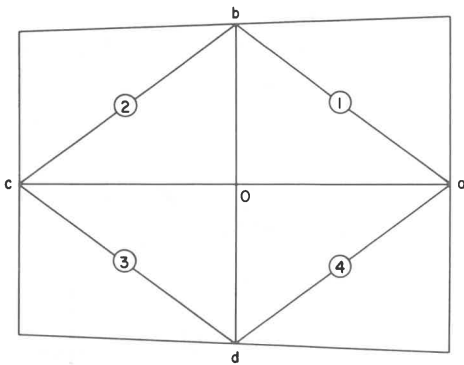
- [1] WANG, C. Y., "Analysis of Nonlinear Fluid-Structure Interaction Transient in Fast Reactors," ANL-78-103 (November, 1978).
- [2] WANG, C. Y., "An Eulerian Method for Analyzing Above-Core Hydrodynamics and Sodium Spillage During a Hypothetical Core Disruptive Accident," Nuclear Technology 51, pp. 332-348 (December, 1980).
- [3] WANG, C. Y., "Analysis of High-Energy Excursions Using the Implicit Continuous-Fluid Eulerian Containment Code - ICECO," Nuclear Technology 51, pp. 400-413 (December, 1980).
- [4] HARLOW, F. H., AMSDEN, A. A., "A Numerical Fluid Dynamic Calculation Method for All Flow Speeds," J. Comp. Phys. 8, p. 197 (1975).
- [5] THORNE, B. J., HOLDRIGE, D. B., "The TOOREZ Lagrangian Rezoning Code," SLA-73-1057, Sandia Laboratory Report (1973).
- [6] WANG, C. Y., "ICECO-CEL: A Coupled Eulerian-Lagrangian Code for Analyzing Primary System Response in Fast Reactors," ANL Report (to be published).
- [7] CHU, H. Y., "A Quasi-Eulerian Method for Analyzing Slug Impact and Coolant Spillage in a Fast Reactor Accident," ANL-79-89 (December, 1979).
- [8] BELYTCHKO, T. B., HSIEH, B. J., "Nonlinear Transient Analysis of Shells and Solids of Revolution by Convected Elements," AIAA, Vol. 12, No. 8, p. 1031 (1974).
- [9] WILKINS, M. L., "Calculation of Elastic-Plastic Flow," UCRL-7322, Rev. 1 (1969).
- [10] ROMANDER, C. M., CAGLIOSTRO, D. J., "Structural Response of 1/20-Scale Models of the Clinch River Breeder Reactor to a Simulated Hypothetical Core Disruptive Accident," SRI Technical Report 4, SRI International (October, 1978).



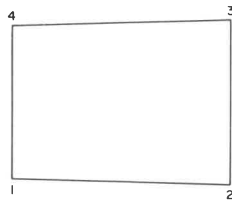
1. Volume of Intersection for Multi-Material-Interaction Analysis.



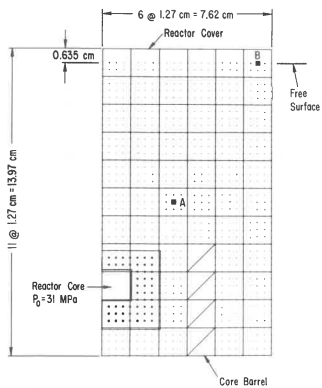
2. Control Volume for Derivation of Radial Momentum Equation.



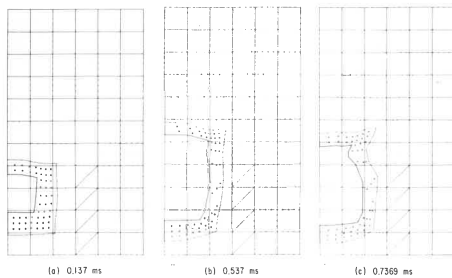
3. Zone Configuration for Finite-Difference Equations.



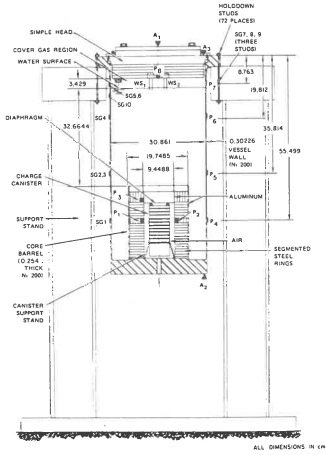
4. Numbering Scheme for Calculating Node Forces of a Typical Element.



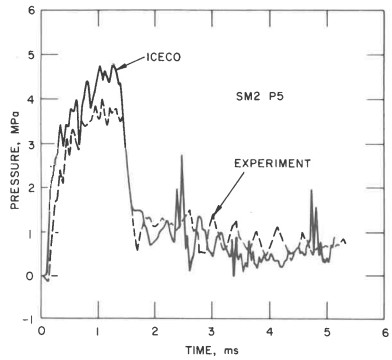
5. Initial Configuration for Two-Material Interaction Analysis.



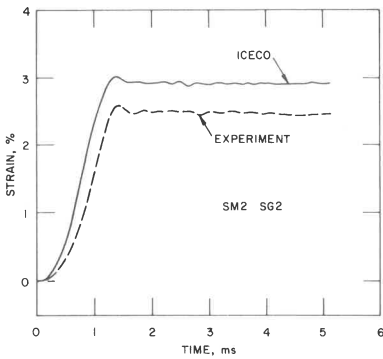
6. Configurations at Three Different Times.



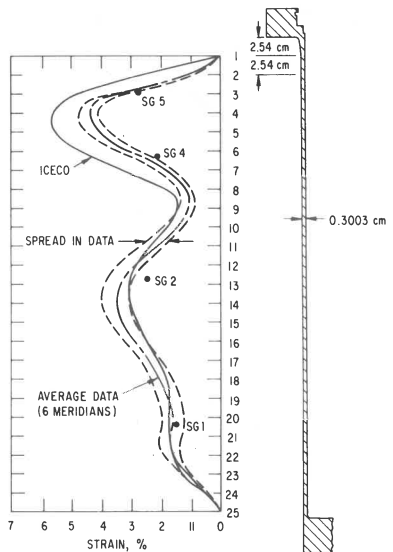
7. The SM-2 Test Model with Instrumentation.



8. Pressure Histories at Gauge P5.



9. Strain Histories at Gauge SG2.



10. Deformable Shape Profile for SM-2 Test.